



Published in final edited form as:

J Phys Chem B. 2015 March 12; 119(10): 3912–3919. doi:10.1021/jp511252y.

Dual-Sensor Fluorescent Probes of Surfactant-Induced Unfolding of Human Serum Albumin

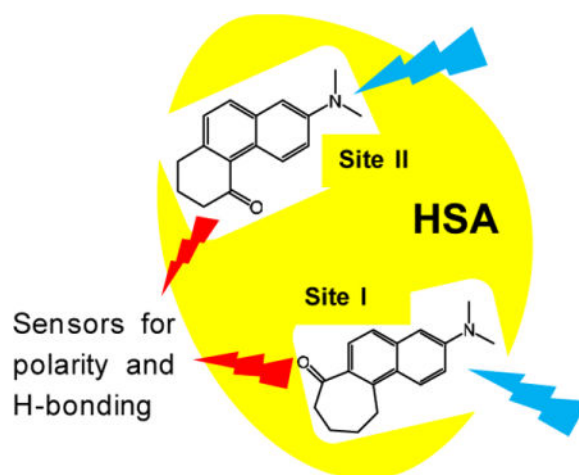
Amy M. Green and Christopher J. Abelt

Department of Chemistry, College of William and Mary, Williamsburg, Virginia, 23185

Abstract

Two extrinsic fluorescent probes, 3-(dimethylamino)-8,9,10,11-tetrahydro-7*H*-cyclohepta[*a*]naphthalen-7-one (**1**) and 7-(dimethylamino)-2,3-dihydrophenanthren-4(1*H*)-one (**2**), are used to probe the unfolding of human serum albumin by sodium dodecyl sulfate (SDS). These probes respond separately to the polarity and H-bond donating ability of their surroundings. Competitive binding experiments show that fluorphore **1** binds to site I (domain IIA) and **2** binds to site II (domain IIIA). The local acidity of **1** in site I is out of the sensing range of **1**, whereas the local acidity of **2** in site II is calculated to be nearly zero on Catalan's solvent acidity index. Both probes show that the first two equivalents of bound SDS result in a decrease in the local polarity of the binding sites. Each subsequent equivalent of SDS gives rise to a dramatic increase in polarity until HSA is saturated with seven molecules of SDS at the end of the specific binding domain. Compound **2** experiences an increase of acidity of 0.10 on Catalan's solvent acidity index through seven equivalents of SDS, but the local acidity for **1** is still out of range. The increase in acidity experienced by **2** is greater than the increase in polarity. This result is consistent with greater exposure of the carbonyl group in **2**, but not the bulk of **2**, to the aqueous solvent in site II of the SDS-saturated HSA complex.

TOC image



SUPPORTING INFORMATION

Supporting Information Available: Molecular Docking results of HSA with **1** and **2**. This material is available free of charge via the Internet at <http://pubs.acs.org>.

Introduction

Human serum albumin (HSA) is the major protein in blood plasma that is responsible for transportation of hydrophobic molecules throughout the body.¹ HSA contains just over 580 amino acids, only one of which is tryptophan and seventeen of which are tyrosines. It has three α -helical domains designated I, II and III. Each of these domains is further divided into subdomains A and B. Small drug molecules are bound primarily at one of two sites (sites I and II as described by Sudlow) that are located in the A subdomains of II and III.^{2,3}

HSA shows high affinity for long alkyl chain anions such as fatty acids and sodium dodecyl sulfate (SDS).⁴ Models suggest that these anions bind at the same sites.⁵ Crystal structures of HSA-fatty acid complexes reveal that there are seven primary fatty acid binding sites of various topologies.^{6,7} Three of these are high affinity sites. Binding at one of these three sites in particular leads to significant conformation changes in the protein. Fatty acid binding can also affect drug binding at sites I and II.

The intrinsic fluorescence of the single tryptophan (Trp 214) and of extrinsic dyes has been used to report on the physiochemical characteristics of the binding sites and in monitoring HSA unfolding.^{8,9} Following the fluorescence of Trp 214 with added SDS^{5,10} reveals four sequential stages or domains during unfolding.¹¹ In order these stages are for specific binding, non-cooperative binding, cooperative binding and saturation binding. These domains have been documented using a variety of extrinsic fluorophores with bovine serum albumin (BSA), which is structurally similar to HSA.^{12–17} The initial interactions of HSA and BSA with SDS provide some stabilization and protection of the protein.^{17,18}

The polarities of the binding sites in the serum albumins have been studied using a variety of fluorescent probes. Most common are molecules that possess an intramolecular charge-transfer excited state (ICT) where the position of the fluorescence emission is affected by the local polarity.^{12–14,16,19–24} Other probes use excited-state intramolecular proton transfer^{15,17,25,26} and (ground-state) proton transfer^{27,28} to elucidate the binding site polarity.²⁹

PRODAN (6-propionyl-2-dimethyaminonaphthalene, Figure 1) was prepared by Weber and Farris as an extrinsic fluorescent probe of BSA.³⁰ PRODAN possesses an ICT excited state, and it has found considerable use as a polarity sensor, especially for lipid bilayers.^{31–35} Drug displacement studies and fluorescent resonance energy transfer studies show that PRODAN binds to site I of HSA.^{36,37} The emission maximum for HSA-bound PRODAN is at 22470 cm^{-1} , an increase of 3400 cm^{-1} from its maximum in water. The addition of palmitic acid to the HSA-PRODAN complex initially leads to an increase in fluorescence intensity. At higher concentrations palmitic acid displaces PRODAN from HSA.

While PRODAN is an often-used polarity sensor, its Stokes shift is also affected by specific H-bonding interactions.^{38–40} In fact, when its solvatochromic shifts are correlated using Catalán's solvent parameters, the coefficient for the polarity term (SPP) is only double that of the solvent acidity (SA) term.^{41,42} The dependence of the emission maximum on both polarity and H-bonding complicates conclusions about its immediate environment.^{32,42}

Recently we have shown that emission intensities of **1** and **2** (Figure 1) are strongly quenched by H-bonding interactions.^{43,44} The correlation between the degree of quenching in an alcohol solvent, defined as $\log(I_{\max}/I)$, and Catalán's solvent acidity parameter SA^{41,45,46} is very linear. As such, the fluorescence intensity of these compounds can be used as sensors of H-bonding ability.^{47,48} PRODAN derivative **1** senses H-bonding in the upper end of the SA scale, whereas PRODAN regioisomer **2** is sensitive to low solvent acidities. The dual-sensing ability of **1** was used recently to characterize the local acidity of its cyclodextrin complex.⁴⁹ In this paper we show that compounds **1** and **2** can be used to shed greater insight into the properties of the HSA binding sites, and, more importantly, changes in the properties of these sites through the specific binding stage of SDS-induced unfolding.

Experimental

Compounds **1** and **2** were prepared previously and sublimed under vacuum before use.^{43,50,51} Essentially fatty acid free HSA was purchased from Sigma-Aldrich. All solvents used in the solvatochromism studies were spectrophotometric grade except for 2-butanol, 2-hexanol and 2-octanol, which were distilled from Na⁰ under N₂ or vacuum. All HSA solutions were made in a 0.05 M phosphate buffer at pH 7.4 in polished water. Fluorescence emission data were collected using a fiber optic system with a 366 nm or 405 nm LED light source and an Ocean Optics Maya CCD detector. Absorption spectra were obtained from the same fiber optic system with a miniature deuterium/tungsten light source. Relative molar absorptivities were determined by the method of standard additions.⁴⁸ Binding isotherm data were generated from the emission spectra of a series of aqueous solutions at 23°C in which the fluorophore concentration was held constant and the HSA concentration was varied. The following procedure was typical: 10–20 µL of a stock solution of fluorophore (ca. 5 mg/10 mL ROH) and a variable volume (0 to 5000 µL) of a stock solution of HSA (ca. 180–360 mg/ 50 mL buffer) were diluted to 5 mL with buffer. Reference solutions of the same concentration of fluorophore in the various alkanols were also prepared. Raw fluorescence intensities were adjusted to account for the detector spectral response and for the conversion from wavelength to wavenumbers.^{48,52} Plots of the integrated intensity ($I = \int I(\tilde{\nu}) d\tilde{\nu}$) vs. [HSA] were fit to equation 1 using non-linear least squares. The limiting intensity of the plot, I_L , is the intensity of the fluorophore-HSA complex, while $f_{\text{H}_2\text{O}}$ is the emission factor ratio between the fluorophore solvated in water and complexed with HSA. This factor accounts for differences in the absorption at the excitation wavelength and in the relative quantum yields (equation 2). The emission center-of-mass was calculated as $\tilde{\nu}_{\text{CM}} = \int I(\tilde{\nu}) \cdot \tilde{\nu} d\tilde{\nu} / \int I(\tilde{\nu}) d\tilde{\nu}$.

$$I = \frac{I_L (f_{\text{H}_2\text{O}} + K [\text{HSA}])}{1 + K [\text{HSA}]} \quad (1)$$

$$f_{\text{H}_2\text{O}} = \frac{\epsilon_{\text{H}_2\text{O}} \cdot \Phi_{\text{H}_2\text{O}}}{\epsilon_{\text{complex}} \cdot \Phi_{\text{complex}}} \quad (2)$$

For the solvent acidity calibrations the integrated emission intensities of **1** and **2** in several reference solvents are converted to emission factor ratios f_{ref} by correcting for the different indices of refraction (equation 3).

$$f_{\text{ref}} = \frac{I_{\text{ref}}}{I_L} \cdot \frac{\eta_{\text{ref}}^2}{\eta_{\text{water}}^2} = \frac{\varepsilon_{\text{ref}} \cdot \Phi_{\text{ref}}}{\varepsilon_{\text{complex}} \cdot \Phi_{\text{complex}}} \quad (3)$$

Rearranging equation 3 gives the ratios of the relative quantum yields of the complex vs. reference solvent (equation 4).

$$\frac{\Phi_{\text{complex}}}{\Phi_{\text{ref}}} = (f_{\text{ref}})^{-1} \frac{\varepsilon_{\text{ref}}}{\varepsilon_{\text{complex}}} \quad (4)$$

The apparent solvent acidities (SA_{app}) in the complexes are determined through equation 5. The slope m is determined from the plot of $-\log(\Phi_{\text{ref}})$ vs. SA.

$$\text{SA}_{\text{app}} = \text{SA}_{\text{ref}} - \frac{\log(\Phi_{\text{complex}}/\Phi_{\text{ref}})}{m} \quad (5)$$

Results and Discussion

Compounds **1** and **2** are very hydrophobic and form strong complexes with HSA. Under conditions where HSA is in great excess, the binding constant for the highest affinity binding site can be determined from the binding isotherm using equation 1. Both **1** and **2** are strongly quenched in water, so the emission factor ratios ($f_{\text{H}_2\text{O}}$) are very small and, in fact, nearly zero with **2**. Figure 2 shows that HSA binds **1** more strongly than **2**. The binding constants are $1.48 \pm 0.07 \times 10^5$ and $5.3 \pm 0.4 \times 10^4 \text{ M}^{-1}$, respectively. These values are smaller than the binding constant of PRODAN with HSA reported by González-Jiménez ($4.2 \times 10^5 \text{ M}^{-1}$), but they bracket the value reported by Panda ($9.2 \times 10^4 \text{ M}^{-1}$).^{36,37} Weber and Farris determined the binding constant of PRODAN with BSA to be 10^5 M^{-1} .³⁰

The binding sites on HSA for **1** and **2** are established through competitive binding studies. The competitive binders for site I and site II are warfarin for site I ($K = 3.4 \times 10^5 \text{ M}^{-1}$) and *S*-naproxen for site II ($K = 3.7 \times 10^6 \text{ M}^{-1}$).⁵³ Both of these drugs have higher affinity towards HSA than does either **1** or **2**. Figure 3 shows that both compounds are displaced by one drug but not the other. For compound **1** the addition of warfarin causes a significant decrease in the intensity without altering $\tilde{\nu}_{\text{CM}}$. On the other hand, naproxen induces only a small but variable change in the intensity, but a decrease of over 200 cm^{-1} in $\tilde{\nu}_{\text{CM}}$. For **2** the addition of naproxen causes an even greater decrease in intensity compared to the effect of added warfarin on **1**-HSA, while the addition warfarin actually leads to an increase in fluorescence. These results suggest that **1** binds to site I, whereas **2** binds to site II. PRODAN is reported to bind to site I.³⁶ PROMEN (6-propionyl-2-methoxynaphthalene), while structurally very similar to PRODAN, is reported to bind to Site II.^{29,54} Results from

molecular docking studies (Supplementary Information) show that both **1** and **2** are bound in Sites I and II. The preferences for one binding site over the other in either case are very small.

Compounds **1** and **2** sense both micropolarity and microacidity. The effective polarity surrounding the fluorophores in the **1**-HSA and **2**-HSA complexes are related to the $\tilde{\nu}_{\text{CM}}$ values, whereas the effective solvent acidities are related to the fluorescence intensities. The Dimroth-Reichert $E_{\text{T}}(30)$ values are the mostly widely used measures of polarity.⁵⁵ The $\tilde{\nu}_{\text{CM}}$ values for **1** and **2** show reasonable linear correlations with this parameter over a range of apolar, aprotic, polar and protic solvents (Figure 4). The fluorescence center-of-mass for **1**-HSA is 21550 cm^{-1} corresponding to an $E_{\text{T}}(30)$ value of 42.1. This polarity is roughly the same as acetone, but smaller than that of isopropanol (48.4) where $\tilde{\nu}_{\text{CM}}$ is 19950 cm^{-1} . For **2**-HSA the $\tilde{\nu}_{\text{CM}}$ value is 18790 cm^{-1} corresponding to an $E_{\text{T}}(30)$ value of 38.4, a polarity similar to that of ethyl acetate. The polarity surrounding **2** in site II is significantly smaller than the polarity of **1** in site I.

The micropolarities of these fluorophores in their HSA complexes are low in comparison to polarities determined for other fluorophore-HSA complexes. Norharmane and an indoloquinolizine derivative show $E_{\text{T}}(30)$ values of 54.9 and 50.3, respectively.^{20,27,28} The micropolarities of BSA-fluorophore complexes have received more attention. Most of these are ICT probes, and $E_{\text{T}}(30)$ values of 39.0,¹³ 39.5,¹⁴ 40.6,²³ 44.2,⁵⁶ 46.0,¹⁶ 46.7⁵⁷ and 48.4¹² have been determined. On the other hand, the 3-hydroxychromone derivative of Demchenko, Klymchenko and Ercelen that binds to site I of HSA shows an $E_{\text{T}}(30)$ value of 37.8 ($E_{\text{T}}^{\text{N}} = 0.22$).^{58,59}

The microacidity-sensing abilities of these compounds are based on the strong quenching that they suffer in protic solvents as a result of H-bonding interactions.^{47,48} The acidity determinations are made by comparing the fluorescence intensities of the complexes and with the intensities of the fluorophores in several reference solvents. The fluorescence intensities of the complexes are given by the limiting intensities from the binding isotherms (I_{L} in eqn 1). The intensities are converted to relative quantum yields by adjusting for the differing molar absorptivities at the excitation wavelengths and the differing indices of refraction. Compound **1** is sensitive to solvent acidity in the range of isopropanol (SA=0.283) to water (SA=1.062), whereas compound **2** responds to acidities less than that of ethanol (SA=0.4). For **1**-HSA the relative quantum yield is nearly as great as that of **1** in isopropanol (data not shown) in which there is little quenching. Because the $\tilde{\nu}_{\text{CM}}$ value for the **1**-HSA complex indicates an effective polarity that is much less than that of isopropanol, it is likely that the effective solvent acidity is also less than that of isopropanol (0.28). That is, the acidity of **1**-HSA is below the range that **1** is able to sense.

The calibration curve for the solvent acidity determination of the **2**-HSA complex is shown in Figure 5. Previously, the range of solvent acidities was determined only with a lower bound of 0.145 (*t*-butanol).⁴⁸ For the current study, the range is extended with references at 0.14 (2-hexanol), 0.88 (2-octanol) and 0.0 (toluene). The y-intercept of the best fit line of the plot of $\log(\Phi_{\text{2-HSA}}/\Phi_{\text{ROH}})$ vs. the solvent acidity parameter determines the effective acidity of the **2**-HSA complex. The intercept is nearly at the toluene reference point, and the

effective acidity is calculated to be 0.01. This number is extremely low, and it is likely that it is only a lower bound. Without H-bonding interactions to deactivate the fluorescence of **2**, the influence of other factors, like the reduced collisional coupling with its surroundings and incomplete dipolar relaxation, will lead to greater fluorescence than in isotropic solution.⁶⁰ Greater fluorescence intensity will translate as a lower effective solvent acidity. On the other hand, the $\tilde{\nu}_{\text{CM}}$ value for the complex (18790 cm^{-1}) is much closer to the $\tilde{\nu}_{\text{CM}}$ value for **2** in toluene (19680 cm^{-1}) than for **2** in 2-octanol (17310 cm^{-1}), suggesting that a low effective SA assignment is warranted. These results suggest that **1** and **2** have very little exposure to the surrounding water.

These two sensors shed light on the beginning of the denaturation process with the detergent SDS in the specific binding range. In this binding domain each molecule of SDS binds successively to HSA until the HSA host is saturated. After that, the SDS molecules bind in a non-cooperative manner. The saturation limit occurs with ~seven molecules of SDS. Figure 6 shows the titration of the HSA complexes with SDS. The mole ratio of the SDS with HSA (based on concentrations) is used as the abscissa, and HSA is used in 100% excess of either fluorophore. The effect of SDS on the fluorescence intensity of the **1**-HSA complex (Figure 6A) is what is often observed with other fluorophores; that is, addition of SDS causes an increase in the fluorescence. The maximum intensity is reached at the end of the specific binding domain. While the fluorescence intensity is increasing, the fluorescence center-of-mass exhibits sigmoidal behavior. It increases slightly through two equivalents of SDS, then it sharply declines until the titration reaches seven equivalents of SDS. The change in the $\tilde{\nu}_{\text{CM}}$ value amounts to 690 cm^{-1} , and $\tilde{\nu}_{\text{CM}}$ shifts to 20450 cm^{-1} . Part of the increase in fluorescence intensity is due to stronger binding. With six equivalents of SDS the binding constant increases to $5.0 \times 10^5 \text{ M}^{-1}$ (Figure 2). The $\tilde{\nu}_{\text{CM}}$ values in the binding isotherm in Figure 2 show that the ratio of bound SDS to HSA does not drop even at low HSA concentrations. If they did, the $\tilde{\nu}_{\text{CM}}$ values would increase according to the behavior seen in Figure 6. Instead, they decrease due to the contribution of free **1** in solution. The remainder of the increase in fluorescence is due to an increase in the quantum yield in the **1**-HSA-SDS_n complex. The fluorescence quantum yield of compound **1** is known to increase with increasing solvent polarity due to optimal formation of the intramolecular charge transfer state. By comparison the $\tilde{\nu}_{\text{CM}}$ value for **1** in isopropanol is 20200 cm^{-1} . Thus, **1** experiences a significant increase in polarity through the specific binding region of denaturation. Because the $\tilde{\nu}_{\text{CM}}$ is still greater than that in isopropanol, the effective acidity surrounding **1** may still be too low to be sensed by **1**. Thus, it is not clear whether the increase in polarity is associated with an increase in solvent exposure.

Even though **2** binds at a different site than **1**, it also experiences a significant increase in polarity ($\tilde{\nu}_{\text{CM}} = 820 \text{ cm}^{-1}$) through the specific binding domain (Figure 6B). In contrast to **1**, the fluorescence intensity decreases precipitously after an initial increase. The decrease in intensity is associated with a decrease in $\tilde{\nu}_{\text{CM}}$, and hence an increase in polarity. The drop in fluorescence intensity is not due to dislodgement by SDS. As with **1**, the binding of **2** by HSA increases three-fold with SDS complexation (from $5.0 \times 10^5 \text{ M}^{-1}$ to $1.5 \times 10^6 \text{ M}^{-1}$, Figure 2). Again, because $\tilde{\nu}_{\text{CM}}$ does not vary during the titration, the stoichiometry of the HSA-SDS_n complex must remain nearly constant. In this case, the drop in fluorescence

intensity can be ascribed to deactivation by H-bonding. When the SDS titration is done in D₂O buffer, the decrease in intensity is significantly less (Figure 6B). Through fourteen equivalents of added SDS **2** experiences a 77% decrease in fluorescence intensity in H₂O vs. only a 41% drop in D₂O. While the change in intensity is less in D₂O than in water, the $\tilde{\nu}_{\text{CM}}$ values show similar sigmoidal behavior. The diminution in quenching in D₂O is consistent with H-bonding being responsible for the increased quenching.

While the D₂O results are definitive for establishing the mode of deactivation for **2** in the HSA-SDS_n complex, there is still the possibility that SDS induces a dislocation of the fluorophore from one binding site to another,⁶¹ one where the second site is more solvent accessible. This possibility can be addressed by titrating ternary complexes, one with a competitive binder in the free primary drug site and the other with a competitive binder that displaces **1** or **2** from their preferred site. Figure 7 shows the SDS titration of **1**-HSA with warfarin and naproxen. The initial $\tilde{\nu}_{\text{CM}}$ for the ternary complexes are $\sim 600 \text{ cm}^{-1}$ lower than for the binary complexes. Warfarin should dislocate **1** from site I. While the decrease in $\tilde{\nu}_{\text{CM}}$ is similar to that without warfarin, its onset is sooner, and it is accompanied by an early onset of the maximum fluorescence intensity at \sim two SDS equivalents. Naproxen should block site II from any dislocation of **1** from site I. Just as is seen in Figure 6 without naproxen, $\tilde{\nu}_{\text{CM}}$ decreases after an initial increase, and it reaches the same minimum at $\sim 20600 \text{ cm}^{-1}$. The increase in fluorescence intensity shows as similar maximum position at \sim five SDS equivalents. While these results are mixed, they suggest that **1** does not dislocate from site I to site II during titration with SDS.

The results are more definitive with the SDS titrations of the **2**-HSA-drug ternary complexes. Figure 8A shows that the **2**-HSA-warfarin complex behaves just like the **2**-HSA complex. Both the intensity and $\tilde{\nu}_{\text{CM}}$ reach a maximum at two equivalents of SDS, then decrease quickly. While the **2**-HSA-naproxen complex shows similar behavior in the fluorescence intensity, the $\tilde{\nu}_{\text{CM}}$ does not show the same initial increase through two equivalents of SDS. These results suggest that **2** does not dislocate from site II to site I during the SDS titration.

From the calibration curve in Figure 5 the increase in quenching for the **2**-HSA-SDS_n complex can be correlated with an increase in SA of 0.10. This value corresponds to a solvent that has stronger H-bond donation than 2-octanol. On the other hand, the $\tilde{\nu}_{\text{CM}}$ value for the complex is 18200 cm^{-1} , but the $\tilde{\nu}_{\text{CM}}$ for **2** in 2-octanol is only 17300 cm^{-1} . The increase in H-bond quenching is greater than the increase in polarity as measured by the $\tilde{\nu}_{\text{CM}}$ value. This disparity suggests that the **2**-HSA-SDS_n complex undergoes significant changes as the number of bound SDS molecules increases. These changes are either in the protein conformation itself or possibly in the orientation of **2** in the binding pocket. Unlike site I which faces subdomain IIIA, the opening to site II is known to be exposed to the solvent.⁶² Either way, the result is much greater exposure of the carbonyl oxygen to the solvent, while the rest of the fluorophore remains fairly protected in a hydrophobic pocket. The increase in effective polarity can be explained in part, if not entirely, by the greater exposure to solvent.

In conclusion, dual fluorescent sensors **1** and **2** reveal facets of the initial phase of denaturation of human serum albumin through the specific binding region. Both sensors show that the respective binding sites become less polar with two equivalents of SDS. With additional equivalents the polarity of both sites increases dramatically until the beginning of the noncooperative binding region. Compound **1**, being sensitive to H-bonding in environments with effective solvent acidity greater than that of isopropanol, is not able to discern whether the polarity increase is due to greater solvent exposure. For compound **2**, the increase in effective polarity is due to solvent exposure as shown by the significant H-bonding induced fluorescence quenching.

Supplementary Material

Refer to Web version on PubMed Central for supplementary material.

Acknowledgments

Acknowledgment is made to the Donors of the American Chemical Society Petroleum Research Fund and to Grant 1R15 089925-01 from the NIH/NHLBI for support of this research.

References

1. Peters, T, Jr. All about albumin: biochemistry, genetics, and medical applications. Academic press; 1995.
2. Sudlow G, Birkett DJ, Wade DN. The Characterization of Two Specific Drug Binding Sites on Human Serum Albumin. *Mol Pharmacol.* 1975; 11:824–832. [PubMed: 1207674]
3. Sudlow G, Birkett DJ, Wade DN. Further Characterization of Specific Drug Binding Sites on Human Serum Albumin. *Mol Pharmacol.* 1976; 12:1052–1061. [PubMed: 1004490]
4. Richieri GV, Anel A, Kleinfeld AM. Interactions of Long-Chain Fatty Acids and Albumin: Determination of Free Fatty Acid Levels using the Fluorescent Probe ADIFAB. *Biochemistry (N Y).* 1993; 32:7574–7580.
5. Gelamo E, Silva C, Imasato H, Tabak M. Interaction of Bovine (BSA) and Human (HSA) Serum Albumins with Ionic Surfactants: Spectroscopy and Modelling. *Biochim Biophys Acta (BBA)-Protein Struct Mol Enzymol.* 2002; 1594:84–99.
6. Ghuman J, Zunszain PA, Petitpas I, Bhattacharya AA, Otagiri M, Curry S. Structural Basis of the Drug-Binding Specificity of Human Serum Albumin. *J Mol Biol.* 2005; 353:38–52. [PubMed: 16169013]
7. Curry, S. X-Ray Crystallography of Albumin. In: Otagiri, M., editor. *Human Serum Albumin - New Insights on its Structural Dynamics, Functional Impacts and Pharmaceutical Applications.* Sojo University Publishing Center; Kumamoto, Japan; 2011. p. 1-29.
8. Hawe A, Sutter M, Jiskoot W. Extrinsic Fluorescent Dyes as Tools for Protein Characterization. *Pharm Res.* 2008; 25:1487–1499. [PubMed: 18172579]
9. Eftink MR. The use of Fluorescence Methods to Monitor Unfolding Transitions in Proteins. *Biophys J.* 1994; 66:482–501. [PubMed: 8161701]
10. Gelamo E, Tabak M. Spectroscopic Studies on the Interaction of Bovine (BSA) and Human (HSA) Serum Albumins with Ionic Surfactants. *Spectrochim Acta, Part A: Mol Biomol Spectrosc.* 2000; 56:2255–2271.
11. Anand U, Jash C, Mukherjee S. Spectroscopic Probing of the Microenvironment in a Protein-Surfactant Assembly. *J Phys Chem B.* 2010; 114:15839–15845. [PubMed: 21077590]
12. Paul BK, Samanta A, Guchhait N. Exploring Hydrophobic Subdomain IIA of the Protein Bovine Serum Albumin in the Native, Intermediate, Unfolded, and Refolded States by a Small Fluorescence Molecular Reporter. *J Phys Chem B.* 2010; 114:6183–6196. [PubMed: 20397640]

13. Mahanta S, Balia Singh R, Bagchi A, Nath D, Guchhait N. Study of protein—probe Complexation Equilibria and protein—surfactant Interaction using Charge Transfer Fluorescence Probe Methyl Ester of N, N-Dimethylamino Naphthyl Acrylic Acid. *J Lumin.* 2010; 130:917–926.
14. Muthusubramanian S, Saha SK. Exploration of Twisted Intramolecular Charge Transfer Fluorescence Properties of Trans-2-[4-(Dimethylamino) Styryl] Benzothiazole to Characterize the protein-surfactant Aggregates. *J Lumin.* 2012; 132:2166–2177.
15. Samanta A, Paul BK, Guchhait N. Spectroscopic Probe Analysis for Exploring probe—protein Interaction: A Mapping of Native, Unfolding and Refolding of Protein Bovine Serum Albumin by Extrinsic Fluorescence Probe. *Biophys Chem.* 2011; 156:128–139. [PubMed: 21514035]
16. Ghosh S, Guchhait N. Chemically Induced Unfolding of Bovine Serum Albumin by Urea and Sodium Dodecyl Sulfate: A Spectral Study with the Polarity-Sensitive Charge-Transfer Fluorescent Probe (E)-3-(4-Methylaminophenyl) Acrylic Acid Methyl Ester. *ChemPhysChem.* 2009; 10:1664–1671. [PubMed: 19466702]
17. Singh RB, Mahanta S, Guchhait N. Destructive and Protective Action of Sodium Dodecyl Sulphate Micelles on the Native Conformation of Bovine Serum Albumin: A Study by Extrinsic Fluorescence Probe 1-Hydroxy-2-Naphthaldehyde. *Chem Phys Lett.* 2008; 463:183–188.
18. Otzen D. Protein-surfactant Interactions: A Tale of Many States. *Biochim Biophys Acta (BBA)- Proteins and Proteomics.* 2011; 1814:562–591. [PubMed: 21397738]
19. Jana S, Dalapati S, Ghosh S, Guchhait N. Potential Charge Transfer Probe Induced Conformational Changes of Model Plasma Protein Human Serum Albumin: Spectroscopic, Molecular Docking, and Molecular Dynamics Simulation Study. *Biopolymers.* 2012; 97:766–777. [PubMed: 22806496]
20. Mallick A, Haldar B, Chattopadhyay N. Spectroscopic Investigation on the Interaction of ICT Probe 3-Acetyl-4-Oxo-6, 7-Dihydro-12H Indolo-[2, 3-a] Quinolizine with Serum Albumins. *J Phys Chem B.* 2005; 109:14683–14690. [PubMed: 16852853]
21. Jana S, Dalapati S, Ghosh S, Guchhait N. Binding Interaction between Plasma Protein Bovine Serum Albumin and Flexible Charge Transfer Fluorophore: A Spectroscopic Study in Combination with Molecular Docking and Molecular Dynamics Simulation. *J Photochem Photobiol A.* 2012; 231:19–27.
22. Ghosh S, Jana S, Guchhait N. Domain Specific Association of Small Fluorescent Probe Trans-3-(4-Monomethylaminophenyl)-Acrylonitrile (MMAPA) with Bovine Serum Albumin (BSA) and its Dissociation from Protein Binding Sites by Ag Nanoparticles: Spectroscopic and Molecular Docking Study. *J Phys Chem B.* 2012; 116:1155–1163. [PubMed: 22126460]
23. Ghosh S, Guchhait N. Fluorescent Probing of Urea-induced Chemical Unfolding of Bovine Serum Albumin by Intramolecular Charge Transfer Fluorescence Probe E-3-(4-Dimethylamino-Naphthalen-1-yl)-Acrylic Acid. *Photochem Photobiol.* 2010; 86:290–296. [PubMed: 20003158]
24. Bhattacharya B, Nakka S, Guruprasad L, Samanta A. Interaction of Bovine Serum Albumin with Dipolar Molecules: Fluorescence and Molecular Docking Studies. *J Phys Chem B.* 2009; 113:2143–2150. [PubMed: 19199686]
25. Maity SS, Samanta S, Sardar PS, Pal A, Dasgupta S, Ghosh S. Fluorescence, Anisotropy and Docking Studies of Proteins through Excited State Intramolecular Proton Transfer Probe Molecules. *Chem Phys.* 2008; 354:162–173.
26. Mukherjee TK, Lahiri P, Datta A. 2-(2'-Pyridyl) Benzimidazole as a Fluorescent Probe for Monitoring protein—surfactant Interaction. *Chem Phys Lett.* 2007; 438:218–223.
27. Ghosh S, Chakrabarty S, Bhowmik D, Kumar GS, Chattopadhyay N. Stepwise Unfolding of Bovine and Human Serum Albumin by an Anionic Surfactant: An Investigation using the Proton Transfer Probe Norharmane. *J Phys Chem B.* 2014
28. Chakrabarty A, Mallick A, Haldar B, Das P, Chattopadhyay N. Binding Interaction of a Biological Photosensitizer with Serum Albumins: A Biophysical Study. *Biomacromolecules.* 2007; 8:920–927. [PubMed: 17315924]
29. Moreno F, González-Jiménez J. Binding of the Promen Fluorescent Probe to Human Serum Albumin: A Fluorescence Spectroscopic Study. *Chem Biol Interact.* 1999; 121:237–252. [PubMed: 10462056]

30. Weber G, Farris FJ. Synthesis and Spectral Properties of a Hydrophobic Fluorescent Probe: 6-Propionyl-2-(Dimethylamino) Naphthalene. *Biochemistry*. 1979; 18:3075–3078. [PubMed: 465454]
31. Parisio G, Marini A, Biancardi A, Ferrarini A, Mennucci B. Polarity Sensitive Fluorescent Probes in Lipid Bilayers: Bridging Spectroscopic Behavior and Microenvironment Properties. *J Phys Chem B*. 2011; 115:9980–9989. [PubMed: 21770447]
32. Adhikary R, Barnes CA, Petrich JW. Solvation Dynamics of the Fluorescent Probe PRODAN in Heterogeneous Environments: Contributions from the Locally Excited and Charge-Transferred States. *J Phys Chem B*. 2009; 113:11999–12004. [PubMed: 19708713]
33. Nitschke WK, Vequi-Suplicy CC, Coutinho K, Stassen H. Molecular Dynamics Investigations of PRODAN in a DLPC Bilayer. *J Phys Chem B*. 2012; 116:2713–2721. [PubMed: 22329741]
34. Mennucci B, Caricato M, Ingrosso F, Cappelli C, Cammi R, Tomasi J, Scalmani G, Frisch MJ. How the Environment Controls Absorption and Fluorescence Spectra of PRODAN: A Quantum-Mechanical Study in Homogeneous and Heterogeneous Media. *J Phys Chem B*. 2008; 112:414–423. [PubMed: 18004838]
35. Cwiklik L, Aquino AJA, Vazdar M, Jurkiewicz P, Pittner J, Hof M, Lischka H. Absorption and Fluorescence of PRODAN in Phospholipid Bilayers: A Combined Quantum Mechanics and Classical Molecular Dynamics Study. *J Phys Chem A*. 2011; 115:11428–11437. [PubMed: 21910413]
36. Moreno F, Cortijo M, González-Jiménez J. The Fluorescent Probe Prodan Characterizes the Warfarin Binding Site on Human Serum Albumin. *Photochem Photobiol*. 1999; 69:8–15. [PubMed: 10063798]
37. Krishnakumar SS, Panda D. Spatial Relationship between the Prodan Site, Trp-214, and Cys-34 Residues in Human Serum Albumin and Loss of Structure through Incremental Unfolding. *Biochemistry (N Y)*. 2002; 41:7443–7452.
38. Cerezo FM, Rocafort SC, Sierra PS, García-Blanco F, Oliva CD, Sierra JC. Photophysical Study of the Probes Acrylodan (1-[6-(Dimethylamino) Naphthalen-2-Yl] Prop-2-En-1-One), ANS (8-Anilino-naphthalene-1-Sulfonate) and Prodan (1-[6-(Dimethylamino) Naphthalen-2-Yl] Propan-1-One) in Aqueous Mixtures of various Alcohols. *Helv Chim Acta*. 2001; 84:3306–3312.
39. Rowe BA, Roach CA, Lin J, Asiago V, Dmitrenko O, Neal SL. Spectral Heterogeneity of PRODAN Fluorescence in Isotropic Solvents Revealed by Multivariate Photokinetic Analysis. *J Phys Chem A*. 2008; 112:13402–13412. [PubMed: 19061326]
40. Homocianu M, Airinei A, Dorohoi DO. Solvent Effects on the Electronic Absorption and Fluorescence Spectra. *J Adv Res Phys*. 2011; 2
41. Catalán J. Toward a Generalized Treatment of the Solvent Effect Based on Four Empirical Scales: Dipolarity (SdP, a New Scale), Polarizability (SP), Acidity (SA), and Basicity (SB) of the Medium. *J Phys Chem B*. 2009; 113:5951–5960. [PubMed: 19344103]
42. Catalan J, Perez P, Laynez J, Blanco FG. Analysis of the Solvent Effect on the Photophysics Properties of 6-Propionyl-2-(Dimethylamino) Naphthalene (PRODAN). *J Fluoresc*. 1991; 1:215–223. [PubMed: 24243072]
43. Everett RK, Nguyen HAA, Abelt CJ. Does PRODAN Possess an O-TICT Excited State? Synthesis and Properties of Two Constrained Derivatives. *J Phys Chem A*. 2010; 114:4946–4950. [PubMed: 20329761]
44. Abelt CJ, Sun T, Everett RK. 2, 5-PRODAN: Synthesis and Properties. *Photochem Photobiol Sci*. 2011; 10:618–622. [PubMed: 21283903]
45. Catalán J, Díaz C. A Generalized Solvent Acidity Scale: The Solvatochromism of o-tert-Butylstilbazolium Betaine Dye and its Homomorph o, o'-Di-tert-butylstilbazolium Betaine Dye. *Liebigs Ann Chem*. 1997:1941–1949.
46. Catalán J, Díaz C. Extending the Solvent Acidity Scale to Highly Acidic Organic Solvents: The Unique Photophysical Behaviour of 3, 6-Diethyltetrazine. *Eur J Org Chem*. 1999:885–891.
47. Green AM, Naughton HR, Nealy ZB, Pike RD, Abelt CJ. Carbonyl-Twisted 6-Acyl-2-Dialkylaminonaphthalenes as Solvent Acidity Sensors. *J Org Chem*. 2013; 78:1784–1789. [PubMed: 22894649]

48. Yoon AH, Whitworth LC, Wagner JD, Abelt CJ. 2, 5-PRODAN Derivatives as Highly Sensitive Sensors of Low Solvent Acidity. *Molecules*. 2014; 19:6415–6427. [PubMed: 24853615]
49. Naughton HR, Abelt CJ. Local Solvent Acidities in β -Cyclodextrin Complexes with PRODAN Derivatives. *J Phys Chem B*. 2013; 117:3323–3327. [PubMed: 23473052]
50. Lobo BC, Abelt CJ. Does PRODAN Possess a Planar Or Twisted Charge-Transfer Excited State? Photophysical Properties of Two PRODAN Derivatives. *J Phys Chem A*. 2003; 107:10938–10943.
51. Silvonek SS, Giller CB, Abelt CJ. Alternate Syntheses of Prodan and Acrylodan. *Org Prep Proced Int*. 2005; 37:589–594.
52. Lakowicz, J. Principles of Fluorescence Spectroscopy. Vol. 2. Kluwer Academic/Plenum Publishers; New York: New York: 1999.
53. Kragh-Hansen U, Chuang VTG, Otagiri M. Practical Aspects of the Ligand-Binding and Enzymatic Properties of Human Serum Albumin. *Biol Pharm Bull*. 2002; 25:695–704. [PubMed: 12081132]
54. González-Jiménez J, Cortijo M. Resonance Energy Transfer between Tryptophan-214 in Human Serum Albumin and Acrylodan, Prodan, and Promen. *Protein J*. 2004; 23:351–355. [PubMed: 15328891]
55. Reichardt, C., Welton, T. Solvents and solvent effects in organic chemistry. Wiley-VCH Verlag GmbH; 2011.
56. Kucherak OA, Richert L, Mély Y, Klymchenko AS. Dipolar 3-Methoxychromones as Bright and Highly Solvatochromic Fluorescent Dyes. *Phys Chem Chem Phys*. 2012; 14:2292–2300. [PubMed: 22237699]
57. Ghosh S, Jana S, Nath D, Guchhait N. Fluorescent Probing of Protein Bovine Serum Albumin Stability and Denaturation using Polarity Sensitive Spectral Response of a Charge Transfer Probe. *J Fluoresc*. 2011; 21:365–374. [PubMed: 20922468]
58. Ercelen S, Klymchenko AS, Mély Y, Demchenko AP. The Binding of Novel Two-Color Fluorescence Probe FA to Serum Albumins of Different Species. *Int J Biol Macromol*. 2005; 35:231–242. [PubMed: 15862861]
59. Ercelen S, Klymchenko AS, Demchenko AP. Novel Two-Color Fluorescence Probe with Extreme Specificity to Bovine Serum Albumin. *FEBS Lett*. 2003; 538:25–28. [PubMed: 12633847]
60. Mallick A, Purkayastha P, Chattopadhyay N. Photoprocesses of Excited Molecules in Confined Liquid Environments: An Overview. *J Photochem Photobiol, C: Photochem Rev*. 2007; 8:109–127.
61. Yamasaki K, Rahman MH, Tsutsumi Y, Maruyama T, Ahmed S, Otagiri M. Circular Dichroism Simulation shows a Site-II-to-Site-I Displacement of Human Serum Albumin-Bound Diclofenac by Ibuprofen. *AAPS Pharm Sci Tech*. 2000; 1:45–54.
62. Curry S. Lessons from the Crystallographic Analysis of Small Molecule Binding to Human Serum Albumin. *Drug Metab Pharmacokinet*. 2009; 24:342–357. [PubMed: 19745561]

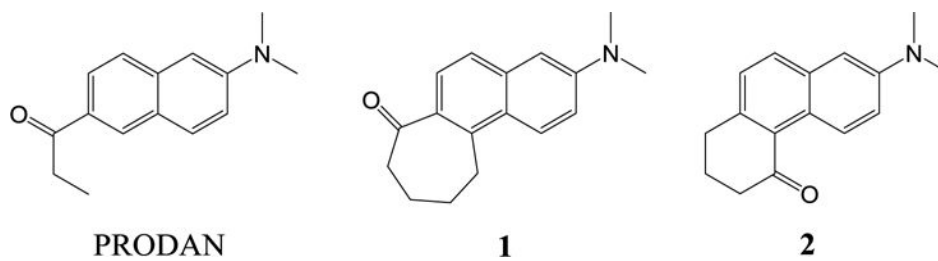


Figure 1.
Structures of PRODAN and derivatives **1** and **2**.

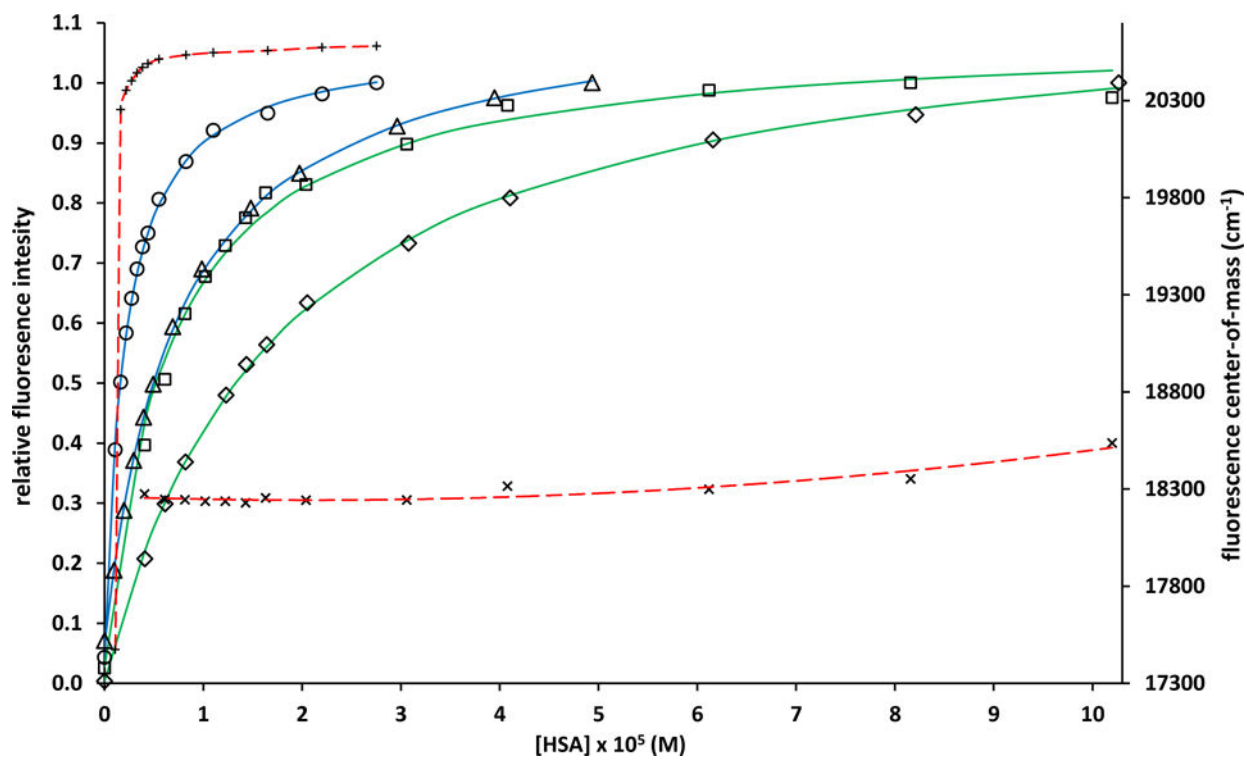


Figure 2. Binding isotherms of **1** (○, —) and **2** (□, —) with HSA and binding isotherms of **1** (△, —) and **2** (◇, —) with HSA and six equivalents of SDS ($[SDS]/[HSA]$ is held constant at ~ 6) along with the corresponding emission center-of-mass: **1** (+, - -) and **2** (x, - -).

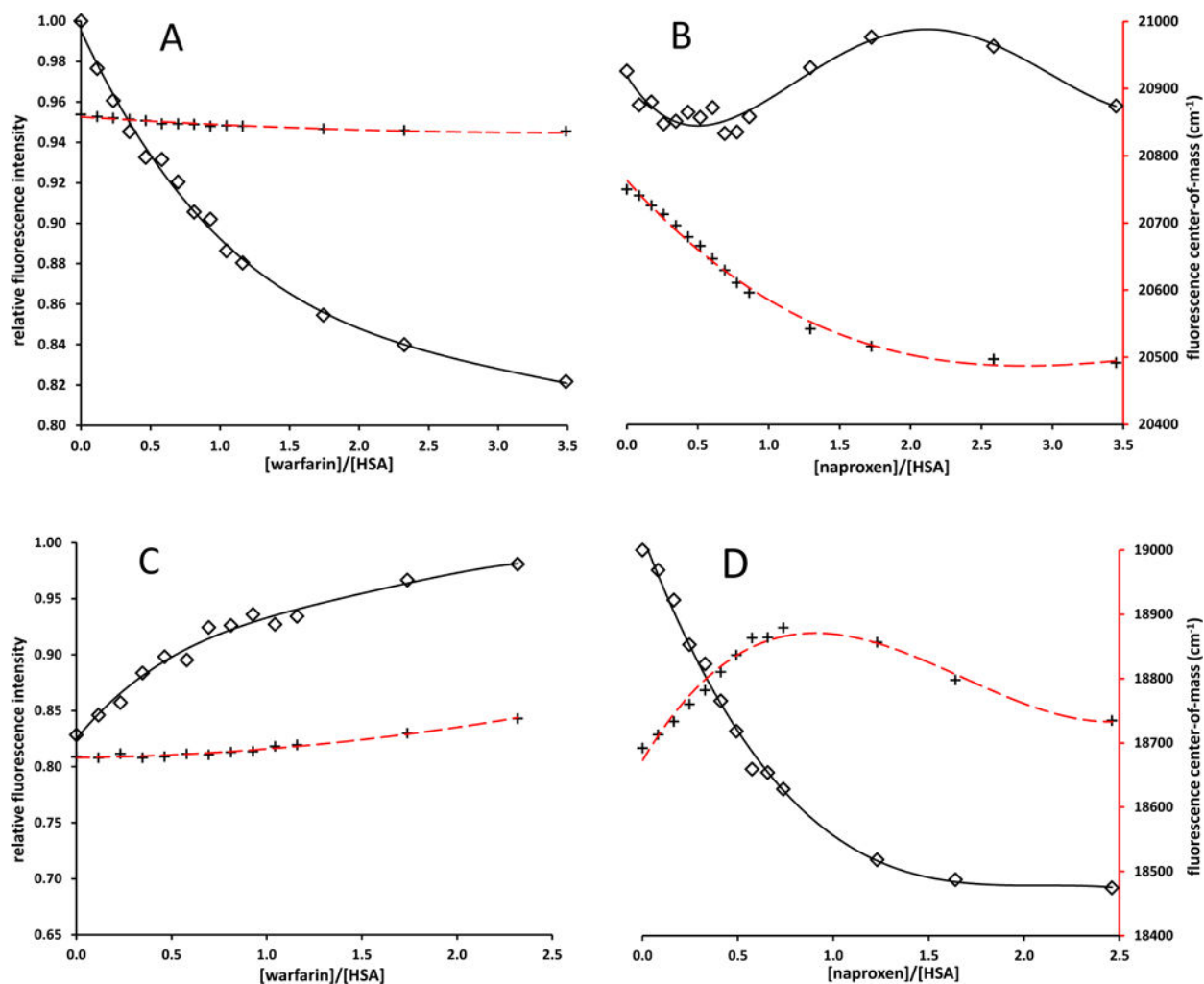


Figure 3. Competitive binding experiments of (A) **1**-HSA with warfarin, (B) **1**-HSA with naproxen, (C) **2**-HSA with warfarin and (D) **2**-HSA with naproxen. HSA is 25 μM and **1** is 2 μM in (A) and (B). HSA is 25 μM and **2** is 6 μM in (C) and (D). Relative intensities are shown in black (, —), while the emission center-of-mass is shown in red (+, - - -).

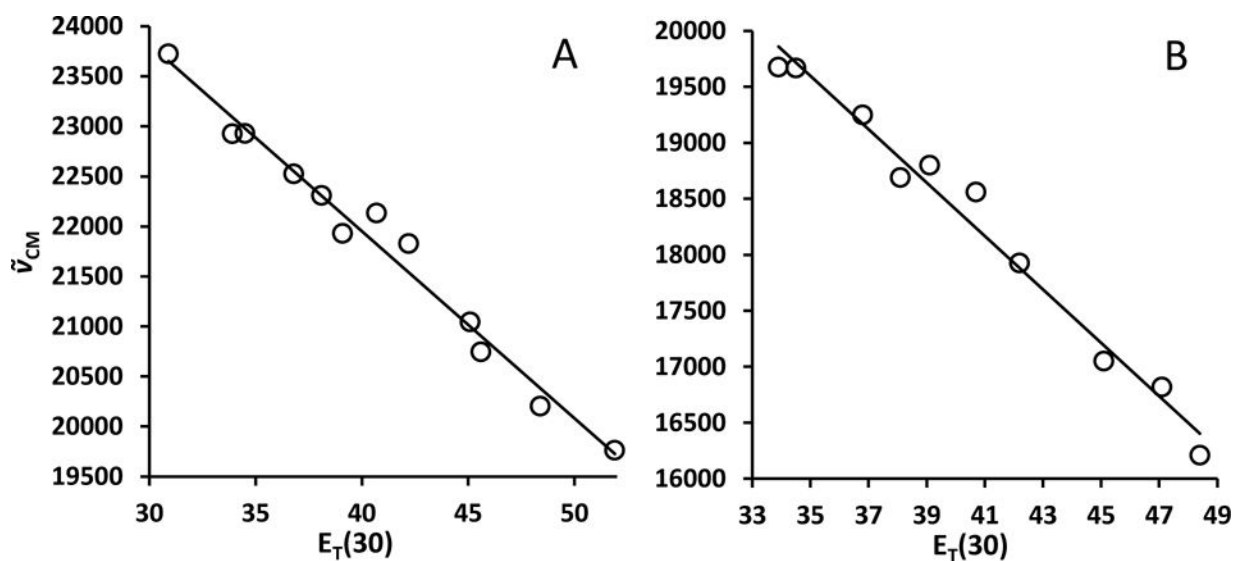


Figure 4.

Plots of (A) $\tilde{\nu}_{CM}$ vs. $E_T(30)$ for **1** in cyclohexane, toluene, chlorobenzene, diethyl ether, chloroform, methylene chloride, ethyl acetate, acetone, dimethyl sulfoxide, acetonitrile, isopropanol and ethanol and (B) $\tilde{\nu}_{CM}$ vs. $E_T(30)$ for **2** in toluene, chlorobenzene, diethyl ether, chloroform, methylene chloride, ethyl acetate, acetone, dimethyl sulfoxide, *sec*-butanol and isopropanol.

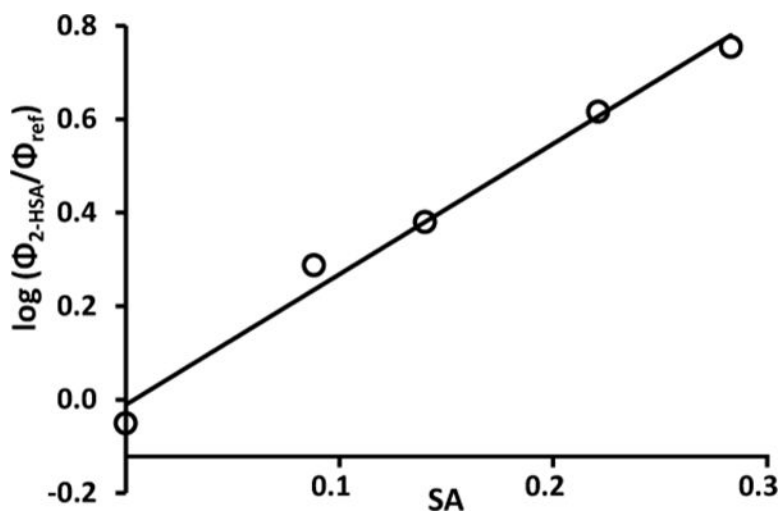


Figure 5. Plot of the logarithm of the ratio of quantum yields between the 2-HSA complex(Φ_{2-HSA}) and five reference compounds (toluene, 2-octanol, 2-hexanol, 2-butanol and isopropanol, Φ_{ref}) vs. their solvent acidity parameters (SA).

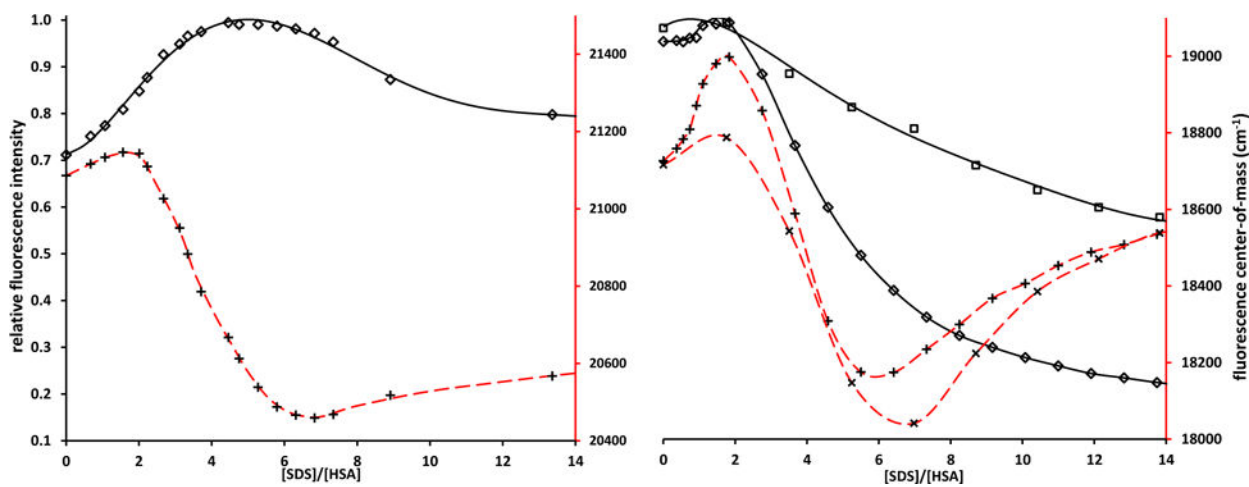


Figure 6.

SDS titration curves: (A), **1**-HSA, fluorescence intensity (○, —) and $\tilde{\nu}_{CM}$ (+, - - -), HSA is 27 μM and **1** is 0.8 μM ; (B), **2**-HSA, fluorescence intensity in phosphate buffer (○, —) and in D_2O buffer (□, —) and $\tilde{\nu}_{CM}$ in phosphate buffer (+, - - -) and in D_2O buffer (×, - - -), HSA is 100 μM and **2** is 6 μM in phosphate buffer and 140 μM and 3 μM , respectively, in D_2O buffer.

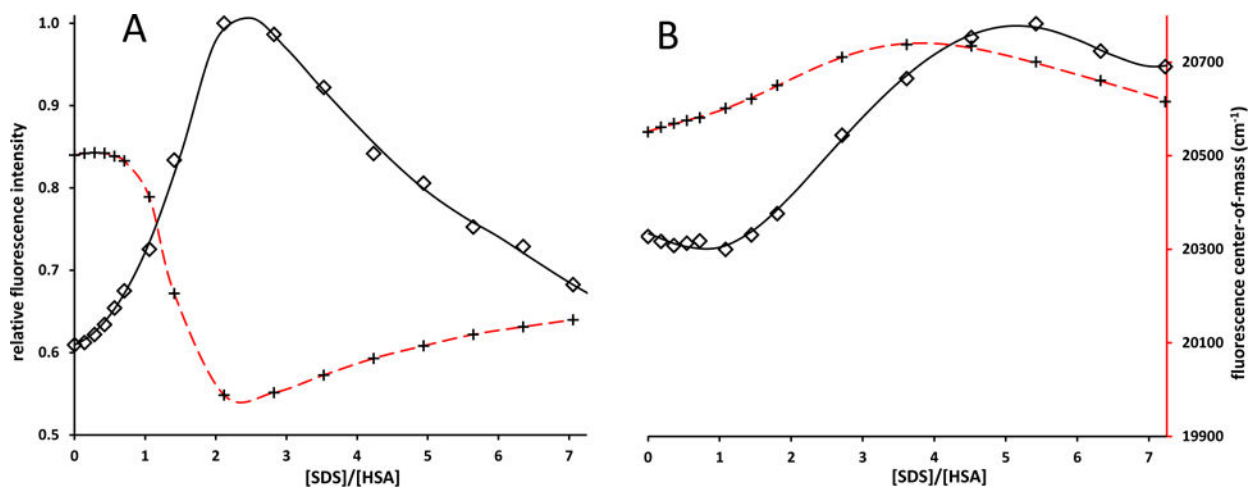


Figure 7. SDS titration curves with competitive binders: (A), **1**-HSA with warfarin, fluorescence intensity (, —) and $\tilde{\nu}_{CM}$ (+, - - -), HSA is 27 μM , **1** is 8 μM and warfarin is 86 μM ; (B), **1**-HSA with naproxen, fluorescence intensity (, —) and $\tilde{\nu}_{CM}$ (+, - - -), HSA is 26 μM , **1** is 8 μM and naproxen is 82 μM .

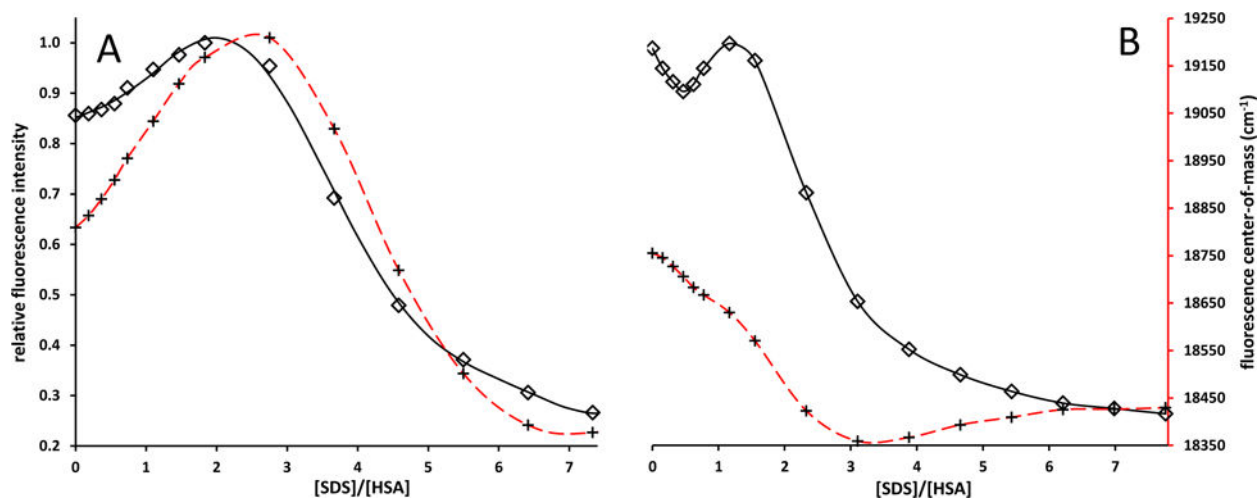


Figure 8.

SDS titration curves with competitive binders: (A), **2**-HSA with warfarin, fluorescence intensity (\diamond , —) and $\tilde{\nu}_{CM}$ ($+$, - - -) HSA is 26 μM , **2** is 12 μM and warfarin is 86 μM ; right: **2**-HSA with naproxen, fluorescence intensity (\diamond , —) and $\tilde{\nu}_{CM}$ ($+$, - - -), HSA is 25 μM , **2** is 12 μM and naproxen is 48 μM .